

K. J. E. Walsh · K.-C. Nguyen · J. L. McGregor

## Fine-resolution regional climate model simulations of the impact of climate change on tropical cyclones near Australia

Received: 25 October 2002 / Accepted: 22 August 2003 / Published online: 12 November 2003  
© Springer-Verlag 2003

**Abstract** Fine-resolution regional climate simulations of tropical cyclones (TCs) are performed over the eastern Australian region. The horizontal resolution (30 km) is fine enough that a good climatological simulation of observed tropical cyclone formation is obtained using the observed tropical cyclone lower wind speed threshold ( $17 \text{ m s}^{-1}$ ). This simulation is performed without the insertion of artificial vortices (“bogussing”). The simulated occurrence of cyclones, measured in numbers of days of cyclone activity, is slightly greater than observed. While the model-simulated distribution of central pressures resembles that observed, simulated wind speeds are generally rather lower, due to weaker than observed pressure gradients close to the centres of the simulated storms. Simulations of the effect of climate change are performed. Under enhanced greenhouse conditions, simulated numbers of TCs do not change very much compared with those simulated for the current climate, nor do regions of occurrence. There is a 56% increase in the number of simulated storms with maximum winds greater than  $30 \text{ m s}^{-1}$  (alternatively, a 26% increase in the number of storms with central pressures less than 970 hPa). In addition, there is an increase in the number of intense storms simulated south of  $30^\circ\text{S}$ . This increase in simulated maximum storm intensity is consistent with previous studies of the impact of climate change on tropical cyclone wind speeds.

2001) concluded that increases in tropical cyclone intensities were “likely, in some regions”. Writing in this report, Giorgi et al. (2001) summarized current understanding of this issue:

1. Little change in the regions of tropical cyclone formation is expected;
2. Changes in numbers could be significant in some regions, mostly tied to possible changes in the behavior of ENSO. A trend that is seen in a number of GCM simulations, to a more “El Niño-like climate” in a warmer world, may lead to tropical cyclone formation that is more similar to that seen in El Niño years than that in the current average climate;
3. There is an emerging consensus that maximum tropical cyclone intensities (i.e. wind speeds) are likely to increase by 5 to 10%. This will be accompanied by increases in peak precipitation rates of 20 to 30%.

These conclusions draw on the results of several studies performed in recent years, from work employing both GCMs (Bengtsson et al. 1995, 1996, 1997; Tsutsui and Kasahara 1996; Krishnamurti et al. 1998; Royer et al. 1998; Yoshimura et al. 1999; Sugi et al. 2002; Tsutsui 2002) and regional modelling results (Walsh and Watterson 1997; Knutson et al. 1998, 2001; Knutson and Tuleya 1999; Walsh and Katzfey 2000; Walsh and Ryan 2000). For projected changes in tropical cyclone intensity, results from theoretical techniques (Emanuel 1987; Holland 1997; Tonkin et al. 1997) have generally supported the conclusions of the modelling studies.

To date, regional model simulations of the effect of climate change on tropical cyclone intensity have mostly used a technique of inserting artificial tropical cyclones (or “bogussing”) into the model, and then comparing the evolution of their intensities under current climate and enhanced greenhouse conditions (e.g. Knutson et al. 1998, 2001; Knutson and Tuleya 1999; Walsh and Ryan 2000). It would be preferable if the simulated storms were generated either by the regional model itself or by

### 1 Introduction

The recent IPCC Third Assessment report on the effects of anthropogenically induced climate change (IPCC

---

K. J. E. Walsh · K.-C. Nguyen · J. L. McGregor  
CSIRO Atmospheric Research, Australia

K. J. E. Walsh (✉)  
School of Earth Sciences, University of Melbourne,  
Victoria 3010, Australia  
E-mail: kevin.walsh@unimelb.edu.au

the global model forcing it, running in climate mode. Knutson and Tuleya (1999) performed one experiment in which the regional model was initialized with weak vortices from the forcing climate model, but this experiment was not a climate simulation and did not produce a simulated climatology of storm numbers. In addition, previous climatological simulations have typically imposed a list of criteria to detect lows in the model that have some of the characteristics of observed tropical cyclones (TCs). For instance, the lows must have a warm core, they must have higher wind speeds in the lower than in the upper troposphere, they must have low-level wind speeds greater than a specified threshold, and so on. Wind speed thresholds used in previous studies have typically been rather lower than the observed tropical storm threshold of  $17 \text{ m s}^{-1}$ . There are good reasons why this is so: a coarser-resolution model like a GCM cannot be expected to generate the tight pressure gradients needed for simulations of reasonable tropical cyclone wind speeds, and so a lower wind speed threshold is needed. However, it would be preferable if the observed threshold could be used for better evaluation of the actual performance of the model.

The resolution of the climatological simulations discussed here is high enough so that this observed threshold can be used and a good simulation of tropical cyclone numbers can still be obtained. This is the first climatological simulation that has this capability. In addition, this simulation does not use any bogussing, enabling an evaluation of the model's native ability to generate strong storms.

Section 2 describes the model and methodology, Sect. 3 gives results, while Sect. 4 discusses the implications and gives a brief summary.

## 2 Materials and methods

### 2.1 Model and domain

The numerical study is carried out using the 3-dimensional CSIRO Division of Atmospheric Research Limited Area Model (DARLAM) of McGregor et al. (1993). DARLAM is a two-time-level, semi-implicit, hydrostatic primitive equation model on an Arakawa staggered C-grid, employing a Lambert conformal projection. The model is semi-Lagrangian, semi-implicit with bi-cubic spatial interpolation used during the horizontal advection. In the vertical, the turbulent mixing is parametrized in terms of stability-dependent K-theory; the shallow cumulus convection scheme of Geleyn (1987) is also used. Cumulus convection is simulated using a modified version of the Arakawa (1972) scheme, as documented in McGregor et al. (1993). Here, a model domain of horizontal grid size  $130 \times 160$  is used with a uniform horizontal resolution of 30 km, with 18 levels in the vertical. This domain is one-way nested within a simulation run on a larger, outer domain at 125 km resolution (Fig. 1), using the method of Davies (1976), modified to use exponentially decreasing weights as suggested by Giorgi et al. (1994). Details of the TC climatology of this outer domain simulation are described in Nguyen and Walsh (2001). The outer domain simulation in turn was nested within a simulation of the CSIRO Mark 2 global coupled ocean-atmosphere GCM (Gordon and O'Farrell 1997), with sea surface temperatures for the 30 km domain interpolated from the GCM values. In the climate change simulation, the

equivalent  $\text{CO}_2$  concentrations are gradually increased. The equivalent  $\text{CO}_2$  concentrations are computed as in Kattenberg et al. (1996):

$$C = C_o \exp(\Delta Q/6.3) \quad (1)$$

where  $C_o$  is the initial concentration (330 ppm) and  $\Delta Q$  is a specified radiative forcing change, here taken following the IPCC/IS92a emission scenario of Kattenberg et al. (1996, see Hirst 1999 for details). The current study analyses simulated results for two time periods: the current climate (represented by the first 30 years, equivalent to 1961 to 1990) and  $3 \times \text{CO}_2$  conditions (i.e. equivalent to  $3 \times \text{CO}_2$  pre-industrial, roughly equivalent to the 30-year period from year 2061 to year 2090).

### 2.2 Detection and tracking methodology

The method used here is the same as that employed in Nguyen and Walsh (2001), with the main difference being that here the observed tropical storm wind speed threshold of  $17 \text{ m s}^{-1}$  is used. Use of this threshold is greatly preferred, but only the high horizontal resolution of this simulation enables this to be done. The other detection criteria used here are either structural criteria used to eliminate intense mid-latitude cyclones or threshold criteria designed to speed up the detection routine by excluding numerous instances of weak, low-level cyclonic vorticity, occurring in fields archived every 12 h.

The criteria are as follows:

1. A vorticity more negative than  $-10^{-5} \text{ s}^{-1}$  (in the Southern Hemisphere);
2. There must be a closed pressure minimum within a radius of 250 km from a point satisfying (1), a distance chosen empirically to give a good geographical association between vorticity maxima and pressure minima; this minimum pressure is taken as the centre of the storm;
3. The total tropospheric temperature anomaly, calculated by summing temperature anomalies at 700, 500 and 300 hPa around the centre of the storm (anomalies from the mean environmental temperature at each level in a band 1200 km east and west and 400 km north and south of the storm), must be greater than zero;
4. The mean wind speed in a region  $800 \times 800 \text{ km}$  square around the centre of the storm at 850 hPa must be greater than at 300 hPa;
5. The temperature anomaly at the centre of the storm at 300 hPa must be greater than at 850 hPa; and
6. The greatest 10 m wind speed observed in the storm at any one time must be at least  $17 \text{ m s}^{-1}$ .

Simulated results are compared with observations from the Joint Typhoon Warning Center (JTWC) best track data.

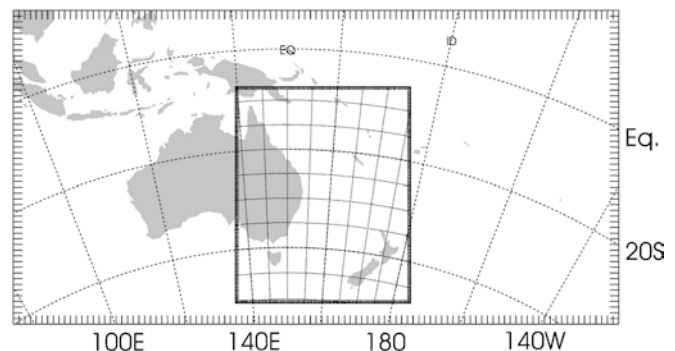


**Fig. 1** DARLAM domains: *inner* 30 km resolution domain, and *outer*, 125 km resolution domain

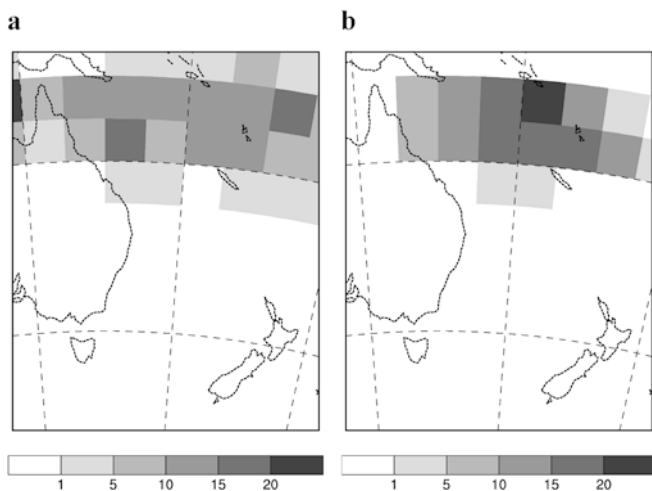
An issue that was addressed in Nguyen and Walsh (2001) was how to best track the storms. In that study, after formation occurred, criteria 3, 4 and 5 were relaxed, and the subsequent evolution of the storm was followed until only criterion 6 was no longer satisfied, in other words when the greatest wind speed in the storm fell below  $17 \text{ m s}^{-1}$ . The rationale for this was that observed tropical cyclones were tracked in a similar manner. The same tracking methodology is used here (termed the “relaxed” detection), but a discussion is also included of the implications for tracking of strictly applying all of the criteria listed all times (“restricted” detection).

### 3 Results

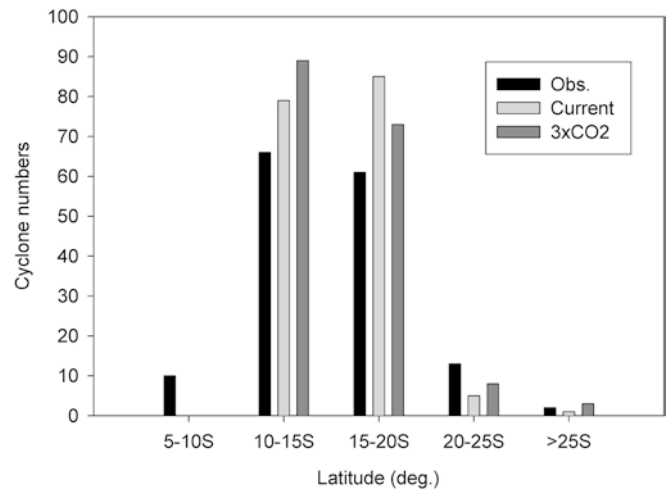
#### 3.1 TC formation and occurrence

Figure 2 shows maps of observed and simulated formation over the eastern Australian region. Simulated TC formation occurs largely at the same latitudes as observed formation. There is somewhat more formation simulated over the open ocean than observed, and rather less near the edges of the domain, where suppression of simulated formation is occurring. This is caused by the DARAM nesting procedure matching fields close to the edge of the 30-km domain with those of the coarser-resolution 125 km domain. Thus TCs in this region are inevitably weaker than in the rest of the 30 km domain and do not reach the  $17 \text{ m s}^{-1}$  threshold.

Figure 3 compares observed and simulated formation for the 30-km resolution simulation for 30 years, January–March, by latitude band. Agreement between observed and simulated formation rates is very good. The two distributions are statistically the same as indicated by the Kolmogorov-Smirnov test of distribution. There is some observed formation in the band 5–10°S that is not simulated. This is due most likely to the northern boundary of the 30-km resolution domain lying within



**Fig. 2** a Observed tropical cyclone formation, January–March, 1967–1996; b simulated TC formation, January–March, 30 year model run



**Fig. 3** Comparison by latitude band over the 30 km domain of January–March observed tropical cyclone formation (black bars); current climate simulated formation (light grey bars); and  $3 \times \text{CO}_2$  conditions simulated formation (dark grey bars). Observations are from the JTWC best track data, 1967–1996

this latitude band and thus suppressing simulated formation.

Results for occurrence (the number of cyclone-days in a given latitude band) are also good (Fig. 4), although the model simulates too much occurrence. A comparison can be made between the occurrence calculated using the “relaxed” detection shown in Fig. 4 and “restricted” detection, where all of the detection criteria are strictly applied at all times during the cyclone track. Figure 5 shows the same comparison as Fig. 4 but using the “restricted” detection. An obvious difference is that the “relaxed” criteria detect more storms at higher latitudes than do the “restricted” criteria. The “relaxed” criteria tend to overestimate storm occurrence at higher latitudes, while the “restricted” criteria underestimate occurrence in those latitudes. At higher latitudes, one

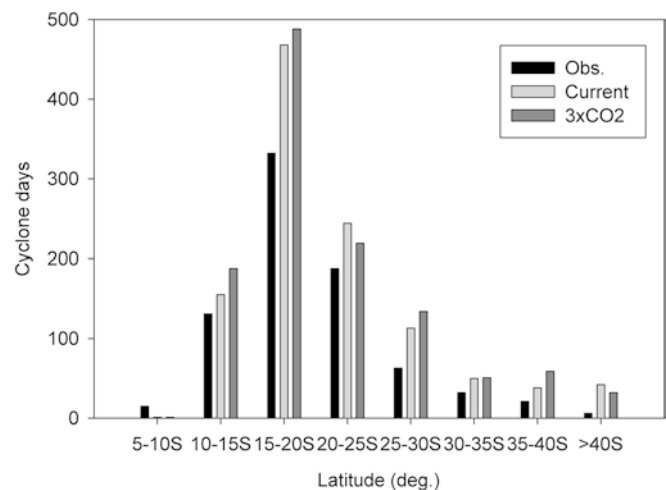


**Fig. 4** The same as Fig. 3 but for occurrence, in cyclone-days

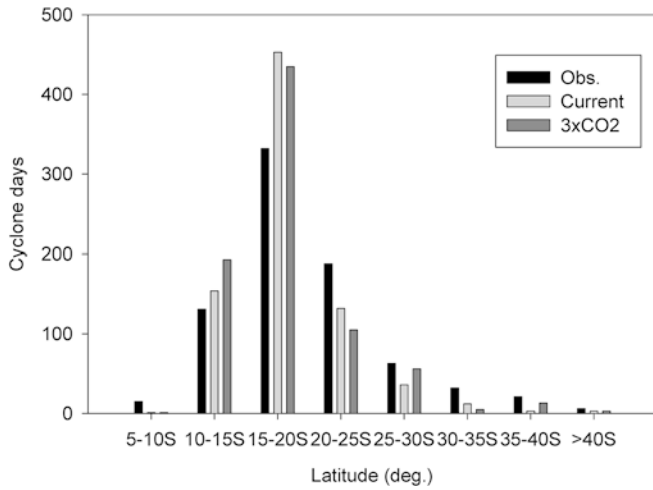


**Fig. 5** The same as Fig. 4 but using the “restricted” detection criteria

way to improve the detection criteria and address the issue of extratropical transition (the transformation of tropical cyclones to extratropical low pressure systems) would be to include an objective criterion for extratropical transition in the detection scheme, along the lines of Hart (2002).

Under  $3 \times \text{CO}_2$  conditions, formation does not change substantially (Fig. 3), although there is an increase in the band 10–15°S, but a decrease in the 15–20°S band. Although these are noticeable differences, the  $1\times$  and  $3 \times \text{CO}_2$  distributions are not statistically significantly different using the Kolmogorov-Smirnov test. Occurrence (Fig. 4) also does not change very much under enhanced greenhouse conditions. There is little systematic difference between the two simulations. In some latitude bands, occurrence increases in a warmer world, while in others it decreases. Previous simulations using this modelling system (Walsh and Katzfey 2000) had produced results that suggested a poleward extension of tropical cyclone occurrence in this region under enhanced greenhouse conditions. In the results shown here, while there appears to be increases in cyclone occurrence in the bands 25–30°S and 35–40°S under enhanced greenhouse conditions (Fig. 4), these are not large and are counterbalanced by decreases in the band 20–25°S. Overall, south of 25°S, there is an increase in occurrence under enhanced greenhouse conditions, consistent with previous results, but these simulations could not really be called conclusive evidence of this effect.

Part of the difficulty of observing this effect in the Australian region was previously discussed in Walsh and Katzfey (2000), but is worth reiterating here. The region east of the Australian continent and south of about 25°S is a region of high climatological wind shear, here defined as the magnitude of the difference of the wind vectors between 200 and 850 hPa. As a result, cyclones often dissipate before traveling very far south in this region. Thus any climate change response may tend to

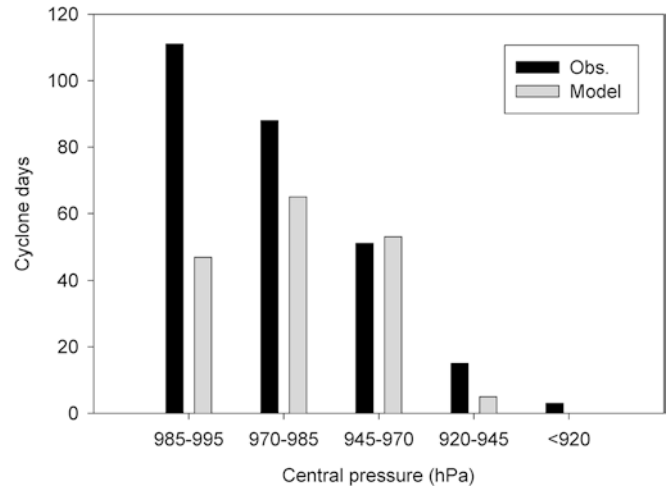


**Fig. 6** Comparison between observed and simulated central pressures. Observations from the Queensland Tropical Cyclone Data Base, 1967–1996, for storms with central pressures less than 995 hPa and travelling south of 10°S and west of 160°E

be swamped by the effect of climatologically high vertical wind shear.

### 3.2 TC intensity

A comparison of observed and simulated intensity is shown in Fig. 6. Here, we compare simulated central pressures rather than wind speeds. There are a large number of storms in the JTWC best track data where intensity is indicated only by tropical storm or hurricane category rather than maximum wind speed or central pressure; data for this comparison shown in Fig. 6 were therefore taken from the Queensland Tropical Cyclone Data Base, compiled by the Australian Bureau of Meteorology, Brisbane, Australia. In these data, storm central pressures are included, but intensities are only indicated by cyclone category rather than wind speed. The resulting comparison (Fig. 6) shows that the model simulates too few weak storms and not enough very strong storms. Note that data is shown only for storms occurring south of 10°S and west of 160°E, as this is the area for which storms are recorded by the Queensland Tropical Cyclone Data Base. This gives different results for total occurrence compared with those shown in Fig. 4, where the results are calculated over a larger area.

One can obtain an indication of how well the model is simulating wind speed by comparing the simulated wind speed for a given central pressure with the conversion relationship between central pressure and maximum wind speed already established for the Queensland forecast region (Bureau of Meteorology 1998). This comparison is shown in Fig. 7 (note that this figure does not include any simulated storms with maximum winds speeds less than  $17 \text{ m s}^{-1}$ ). The model is clearly simulating a lower than observed maximum wind speed for a given central pressure. Even though the model is

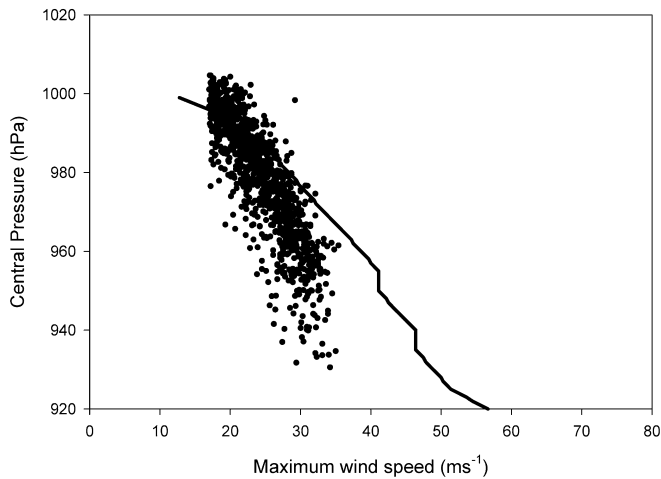


**Fig. 7** Observed relationship between tropical cyclone maximum wind speed and central pressure (*solid line*) compared with simulated TC maximum wind speeds and central pressures (*dots*). Observed relationship interpolated from data given in Bureau of Meteorology (1998)

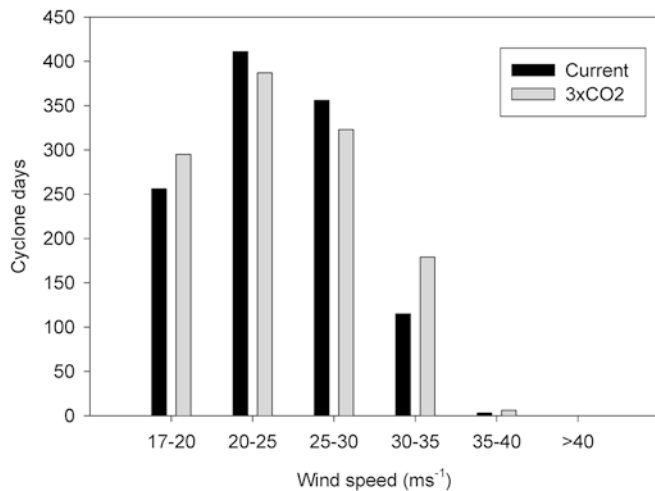


**Fig. 8** Comparison between simulated wind speed distribution for current climate (*white bars*) and enhanced greenhouse conditions (*grey bars*)

implemented at a resolution of 30 km, it still does not simulate a pressure gradient close to the centre of the storm that is comparable to that seen in reality. Thus although the storm central pressures can be quite deep (compare Fig. 6), the wind speeds are rather lower than observed.

Having said this, a comparison between simulated wind speeds in the current climate and under  $3 \times \text{CO}_2$  conditions is shown in Fig. 8. Larger numbers of the strongest storms occur under enhanced greenhouse conditions, consistent with previous results. A similar comparison for central pressures is shown in Fig. 9. These numbers represent a 56% increase in the number of storms with simulated maximum winds greater than  $30 \text{ m s}^{-1}$  and a 26% increase in the number of storms

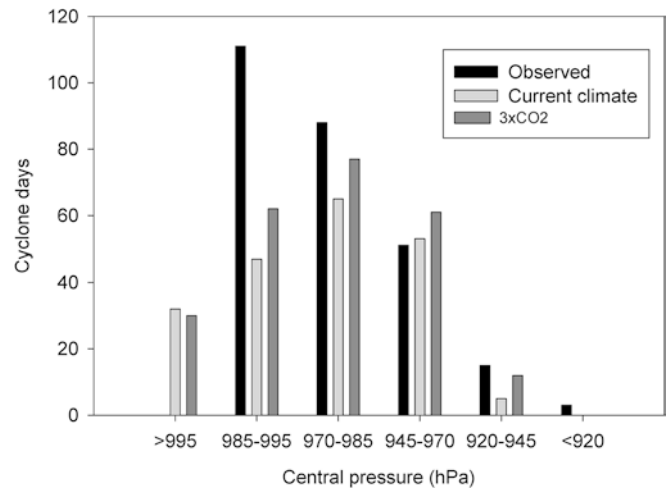


**Fig. 9** Comparison between observed (*black*), current climate simulated (*light grey*) and  $3 \times \text{CO}_2$  climate simulated (*dark grey*) central pressures of storms for the region south of  $10^\circ\text{S}$  and west of  $160^\circ\text{E}$

with central pressures less than 970 hPa. These results are consistent with our current understanding of the effect of climate change on maximum tropical cyclone intensities (Giorgi et al. 2001).

### 3.3 Causes of intensification and dissipation

It is well known that changes in intensity of tropical cyclones are closely related to prevailing conditions of vertical wind shear and sea surface temperature (SST; DeMaria 1996; Gallina and Velden 2002). Figure 10 shows changes between the current and  $3 \times \text{CO}_2$  runs for these two variables, as well as rainfall, which is related to the model's ability to generate incipient convective disturbances. Increases in SST (Fig. 10a) are mostly  $1.5\text{--}2^\circ\text{C}$  over the model domain. All other things being equal, this should lead to a modest increase in maximum storm intensity in this region. Similarly, there is some increase in rainfall in the enhanced greenhouse run north of  $17^\circ\text{S}$  (Fig. 10b), which would suggest better convective conditions for storm formation and thus perhaps more precursor disturbances. The vertical wind shear pattern (Fig. 10c), however, shows mostly decreases in shear north of about  $17^\circ\text{S}$ , but increases south of this latitude. Changes are mostly small but in some locations approach  $2 \text{ m s}^{-1}$ , which may be large enough to cause some consistent differences in tropical cyclone formation (Shapiro 1987). Thus simulated formation north of  $17^\circ\text{S}$  would be increased in the enhanced greenhouse run, whereas south of this latitude it would be generally decreased. When formation numbers are partitioned by the  $17^\circ\text{S}$  meridian, however, little change in formation in enhanced greenhouse conditions is seen (not shown).

The modelling system here has some ability to replicate observed relationships between intensity, SST and

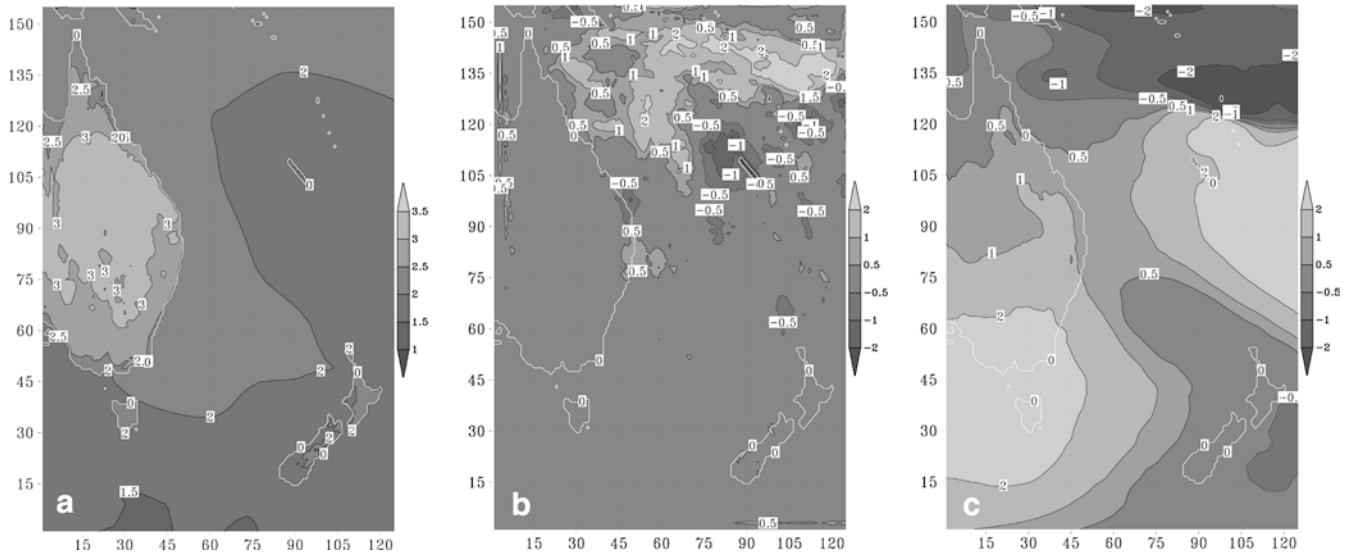


**Fig. 10** Change in mean between current climate and  $3 \times \text{CO}_2$  climate simulation, for **a** SST; **b** precipitation; and **c** vertical wind shear. Contour intervals  $0.5 \text{ } ^\circ\text{C}$ ,  $0.5 \text{ mm day}^{-1}$  and  $0.5 \text{ ms}^{-1}$  respectively

shear. Figure 11 shows plots of the relationship between change in central pressure, vertical wind shear and SST over the subsequent 24 h for the current climate simulation (Fig. 11a), and the same over 48 h (Fig. 11b). Here we have excluded storms that are in the process of landfall, and also storms south of  $30^\circ\text{S}$ , where extratropical influences on intensity are more likely to occur. These plots are created by an inverse distance method that interpolates  $z$  values for an evenly spaced  $xy$  grid from  $xyz$  triplet data.

There is considerable scatter in the data, but the results do suggest that intensification (decrease in central pressure) is favoured for low values of shear and high values of SST. The results are particularly pronounced over 48 h (Fig. 11b). Multiple regression analysis shows that both of these relationships are highly statistically significant using the  $F$  test, but because of the scatter the percentage of variance explained is not high ( $r^2$  approximately 0.15 in both cases).

Some features of Fig. 11b are of interest. Rapid intensification is possible for values of shear less than  $10 \text{ m s}^{-1}$  and SSTs greater than about  $28 \text{ } ^\circ\text{C}$ . Shear begins to cause substantial decreases in storm intensity for shear values slightly greater than  $10 \text{ m s}^{-1}$ . In comparison, Gallina and Velden (2002) found this “critical” shear value above which observed tropical cyclones start to fill to be  $7\text{--}8 \text{ m s}^{-1}$  in the Atlantic and  $9\text{--}10 \text{ m s}^{-1}$  in the western north Pacific. In our simulations, maximum storm weakening occurs for shear approaching  $20 \text{ m s}^{-1}$ . In contrast, for storms experiencing very high shear values ( $> 25 \text{ m s}^{-1}$ ), some storm intensification may even take place. This may indicate some influence of extratropical conditions, as these particular storms are at latitudes south of the tropics, with most close to  $30^\circ\text{S}$ .

Turning to those storms that travel south of  $30^\circ\text{S}$ , Fig. 12 shows a similar plot, but only for 24 h, as few

storms last more than 48 h at these latitudes, either by dissipating, striking land (New Zealand) or hitting one of the model boundaries. Figure 12 shows that there is a similar relationship to that of Fig. 11, but with a couple of important differences. Decreases in intensity (increases in central pressure) are strong for wind shear values approaching  $20 \text{ m s}^{-1}$ , but usually only if the SST is also low. Regression analysis again shows a strong relationship between increases in storm central pressure and the prevailing SST and wind shear, but this is due mostly to the SST, with correlations between SST and storm dissipation very strong ( $r = 0.63$ ), while the relationship of changes in central pressure to shear is much weaker ( $r = 0.14$ ). Overall, multiple regression gives a strongly significant relationship for predictions of increases in storm central pressure using the prevailing SST and wind shear, with  $r^2 = 0.41$ , mostly due to the effect of SST.

Observed tropical cyclone damage increases non-linearly with intensity (Pielke and Landsea 1998), with major hurricanes (Saffir-Simpson category 3 or higher) accounting for 83% of all Atlantic hurricane damage, despite only comprising 21% of all landfalling tropical cyclones in this region. While acknowledging that the simulation of wind speeds in this study is inadequate, we examine the latitudinal distribution of storms with central pressures less than  $965 \text{ hPa}$  (equivalent to Saffir-Simpson category 3 or greater) in the current and enhanced greenhouse climates. This is shown in Fig. 13. While there are some latitudinal bands where the occurrence of these storms increases in a warmer world ( $15\text{--}20^\circ\text{S}$ ;  $30\text{--}40^\circ\text{S}$ ), there are also some where it decreases ( $20\text{--}30^\circ\text{S}$ ;  $> 40^\circ\text{S}$ ). This may be partially explained by comparing this result to Fig. 10. It is noted that in the region  $20\text{--}30^\circ\text{S}$  vertical wind shear is greater in the enhanced greenhouse simulation, which would tend to oppose the increase in TC

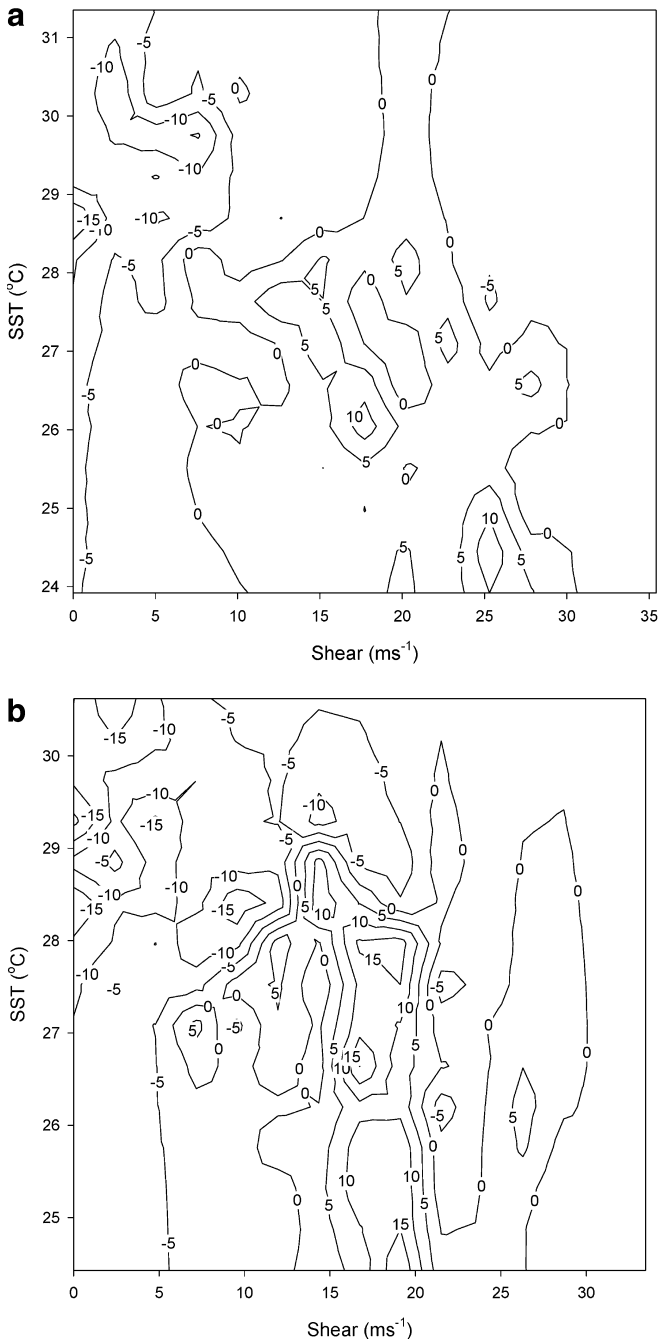


**Fig. 11** Change in central pressure (hPa) as a function of vertical wind shear ( $\text{ms}^{-1}$ ) and SST ( $^{\circ}\text{C}$ ), for **a** 24 h; and **b** 48 h

intensity caused by increased SSTs at these latitudes. In general, the increased SSTs in the enhanced greenhouse simulation do not appear to be causing a systematic poleward enhancement of TC intensity in this region in a warmer world. However, the strong relationship between dissipation and lower SSTs south of  $30^{\circ}\text{S}$  accounts for the increase in intense storm days in these latitudes under enhanced greenhouse conditions. Changes in stability over this region, while not explicitly examined here, may also have an effect (Sugi et al. 2002).

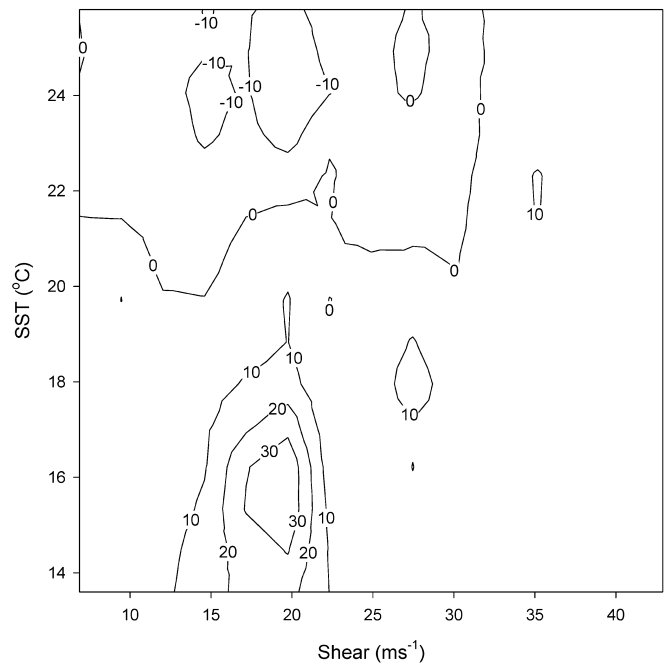


**Fig. 12** The same as Fig. 11a but for storms traveling south of  $30^{\circ}\text{S}$

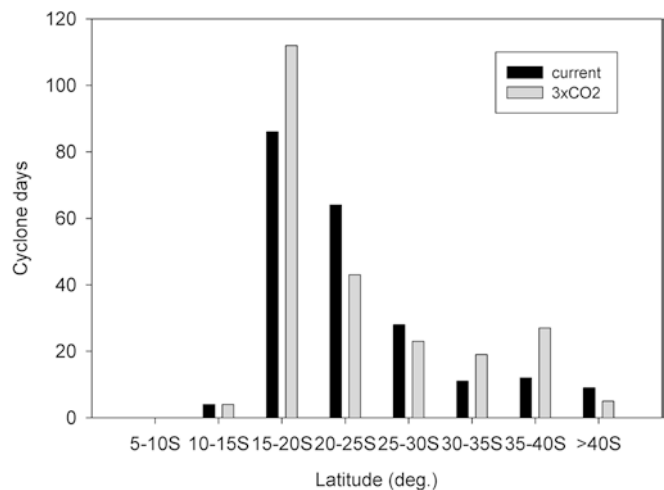


**Fig. 13** Distribution by latitude of all simulated storms with a central pressure of less than 965 hPa, for current climate simulation (black bars) and enhanced greenhouse conditions (grey bars)

### 3.4 Interannual variability

Interannual variations in observed tropical cyclone formation in the simulated region are strongly associated with variations in ENSO (e.g. Basher and Zheng 1995), so it is of interest to determine the model's ability to simulate this interannual variability. While the modeling system does have some ability to generate interannual variations similar to ENSO, it does not have a similar ability to generate interannual variations in tropical cyclone formation similar to those observed. Correlations were calculated between the interannual

variation of TC formation and the indices of ENSO generated by the forcing GCM and outer domain limited area model (see Nguyen and Walsh 2001, Fig. 3). Correlations were not significant between interannual TC formation and model-generated Southern Oscillation Index (SOI), Niño 3 or Niño 4 SST indices. Nor were simulated La Niña years (defined in the model as  $\text{SOI} > 2$ ) more likely to exhibit TC formation in this region than El Niño years (defined in the model as  $\text{SOI} < -2$ ), as observed. We conclude that although the model has a good simulation of average TC formation, the simulated ENSO forcing from the outer domain LAM is too weak to affect simulated interannual formation in the inner, 30-km resolution LAM domain. Better results might be obtained with the new generation of GCMs that simulate much larger and more realistic ENSO variations (e.g. HADCM3, Gordon et al. 2000; CSIRO Mk3, Gordon et al. 2002).

#### 4 Discussion and conclusion

As mentioned earlier, almost all previous modelling studies have used a windspeed detection threshold for tropical cyclone-like vortices that is less than the observed tropical cyclone threshold of  $17 \text{ m s}^{-1}$ . One of the advantages of the modelling system described here is that the horizontal resolution is fine enough that it is not necessary to specify a lower than observed threshold. Nevertheless, a lower than observed threshold is probably more appropriate for a relatively coarse resolution model, as we know a priori that the model will not be able to simulate the extreme winds observed in tropical cyclones. In principle, “resolution-appropriate” detection criteria for GCMs could be diagnosed from reanalyses that have an excellent representation of tropical cyclone structure. In practice, current reanalyses are probably not adequate for this purpose (e.g. Fiorino 2002). Even so, despite the lack of generally accepted “resolution-appropriate” threshold detection criteria, insights into the effect of climate change on tropical cyclones can still be obtained from GCMs. Most global models predict little or no change in the regions of initial tropical cyclone formation, and this result may be robust to changes in the exact values of detection thresholds. A test was conducted of the sensitivity of formation numbers to the exact value of the wind speed threshold. It could be argued that a grid resolution of 30 km is still too coarse to use the observed  $17 \text{ m s}^{-1}$  threshold and that a lower value would be more appropriate to the resolution. Using a threshold of  $14 \text{ m s}^{-1}$  instead, detected TC numbers increased by 41%, which indicates significant sensitivity to this parameter and may indicate that the model is still generating too many TCs compared with observations.

The present study suggests that one way to avoid the issue of resolution-dependent thresholds would be to use a combination of global models and regional climate models, implemented over the individual tropical

cyclone formation basins, to address the issue of the effect of climate change on tropical cyclones. Regional climate models will be run at even finer resolutions in the future, giving more confidence in their predictions, since even a climate model of 30-km horizontal resolution such as used here is fairly coarse to simulate a tropical cyclone.

An additional limitation of a regional model is that its climatology is to a large extent dependent on that of the forcing global model, and this would also be the case for simulated TCs. Nguyen and Walsh (2001) note that the SST pattern in the forcing GCM tends towards a more El Niño-like state in the enhanced greenhouse simulation, with temperature rising more in the eastern Pacific than in the west. There is a strong relationship between ENSO and tropical cyclone numbers close to the Australian coast, with numbers less during El Niño years and more during La Niña years (Hastings 1990). This would tend to reduce tropical cyclone numbers in the simulation in the limited area model domain used here. Nguyen and Walsh (2001) found that simulated TC numbers decreased slightly under enhanced greenhouse conditions west of  $170^\circ\text{E}$ , while numbers stayed about the same east of this meridian. In the current simulation, this behaviour is not seen, with formation remaining about the same both west and east of this meridian. One explanation may be that the interannual forcing from the GCM may be too weak, as mentioned earlier. This may also be due to the general increase in convection in a warmer world in the formation region, whereas in the forcing GCM in the same location, precipitation decreases. In contrast, in the GCM simulation by Sugi et al. (2002), the SSTs increased more in the western Pacific under enhanced greenhouse conditions than they did in the east. This was associated with a decrease in simulated TC formation in the southwest Pacific region, but Sugi et al. (2002) ascribed this to a general stabilization of the tropical atmosphere rather than to the change in the SST pattern.

The issue of whether warmer SSTs would extend the poleward occurrence of tropical cyclones (as opposed to formation regions) in a warmer world was also examined. The results shown did not constitute strong evidence of this effect. It is recommended that this issue be examined further in other regions of the globe, and that theoretical techniques be developed to address the topic, as well as the related issue of possible changes in extratropical transition characteristics in a warmer world.

In summary, 30-km horizontal resolution climate simulations were implemented over the eastern Australian region and used to examine both the model’s ability to simulate the current climate of tropical cyclones in this region and any changes in a warmer world. The model has a very good simulation of tropical cyclone formation in the current climate and a reasonable simulation of occurrence. The simulated distribution of storm central pressures is reasonable, although because the model simulates weaker than observed pressure gradients close to the storm centre, the model wind



speeds are considerably weaker than observed. Under enhanced greenhouse conditions, numbers of tropical cyclones formed and their regions of formation do not change much. Occurrence also does not change substantially, although there is an increase in the number of intense storms simulated south of 30°S. Overall, there is a 56% increase in the number of storms with simulated maximum winds greater than 30 m s<sup>-1</sup>, or a 26% increase in the number of storms with central pressures less than 970 hPa, a result consistent with previous studies suggesting an increase in tropical cyclone maximum intensities in a warmer world.

**Acknowledgements** The authors would like to thank the State Government of Queensland, particularly the Department of Natural Resources and Mines, and CSIRO for supporting this work. Jack Katzfey, Mike Fiorino and an anonymous reviewer made comments that improved the work.

## References

- Arakawa A (1972) Design of the UCLA general circulation model. Numerical simulation of weather and climate. Techn Rep 7, Department of Meteorology, University of California, Los Angeles, USA
- Basher RE, Zheng X (1995) Tropical cyclones in the southwest Pacific: spatial patterns and relationships to Southern Oscillation and sea surface temperature. *J Clim* 8: 1249–1260
- Bengtsson LM, Botzet M, Esch M (1995) Hurricane-type vortices in a general circulation model. *Tellus* 47A: 175–196
- Bengtsson L, Botzet M, Esch M (1996) Will greenhouse gas induced warming over the next 50 years lead to higher frequency and greater intensity of hurricanes? *Tellus* 48A: 57–73
- Bengtsson L, Botzet M, Esch M (1997) Numerical simulation of intense tropical storms. In: Diaz HF, Pulwarty RS (eds) *Hurricanes: climate and socioeconomic impacts*. Springer, Berlin Heidelberg, New York, pp 67–92
- Bureau of Meteorology (1998) Tropical cyclone warning directive. Available from Bureau of Meteorology, Queensland Regional Office, GPO Box 413, BRISBANE QLD 4001, Australia
- Davies HC (1976) A lateral boundary formulation for multi-level prediction models. *Q J R Meteorol Soc* 102: 405–418
- DeMaria M (1996) The effect of vertical wind shear on tropical cyclone intensity change. *J Atmos Sci* 53: 2076–2087
- Emanuel KA (1988) The maximum intensity of hurricanes. *J Atmos Sci* 45: 1143–1155
- Fiorino M (2002) Analysis and forecasts of tropical cyclones in the ECMWF 40-year reanalysis (ERA-40). *Proc 25th Conf Hurricanes and Tropical Meteorology*, San Diego, 29th April–3rd May, 2002, American Meteorological Society, pp 261–264
- Gallina GM, Velden CS (2002) Environmental wind shear and tropical cyclone intensity change using enhanced satellite derived wind information. *Proc 25th Conf Hurricanes and Tropical Meteorology*, San Diego, 29th April–3rd May, 2002, American Meteorological Society, pp 172–173
- Geleyn JF (1987) Use of a modified Richardson number for parameterizing the effect of shallow convection. In: Matsuno T (ed) *Short- and medium-range numerical weather prediction. Spec Vol J Meteorol Soc Japan*, pp 141–149
- Giorgi F, Brodeur CS, Bates GT (1994) Regional climate change scenarios over the United States produced with a nested regional climate model. *J Clim* 7: 375–399
- Giorgi F, Hewitson B, Christensen J, Hulme M, von Storch H, Whetton P, Jones R, Mearns L, Fu C (2001) Regional climate change information – evaluation and projections. In: Houghton JT, Ding Y, Griggs DJ, Noguera M, van der Linden PJ, Dai X, Maskell K, Johnson CA (eds) *Climate change 2001 – the scientific basis*. Intergovernmental Panel on Climate Change, Cambridge University Press, Cambridge, UK, pp 583–638
- Gordon C, Cooper C, Senior CA, Banks H, Gregory JM, Johns TC, Mitchell JFB, Wood RA (2000) The simulation of SST, sea ice extents and ocean heat transports in a version of the Hadley Centre coupled model without flux adjustments. *Clim Dyn* 16: 147–168
- Gordon HB, O’Farrell SP (1997) Transient climate change in the CSIRO coupled model with dynamic sea ice. *Mon Weather Rev* 125: 875–907
- Gordon HB, Rotstain LD, McGregor JL, Dix MR, Kowalczyk EA, O’Farrell SP, Waterman LJ, Hirst AC, Wilson SG, Watterson IG, and Elliott TI (2002) The CSIRO Mk 3 Climate Systems Model, CSIRO Atmospheric Research Techn Pap 60
- Hastings PA (1990) Southern Oscillation influences on tropical cyclone activity in the Australian/south-west Pacific region. *Int J Climatol* 10: 291–298
- Hart R (2002) A cyclone phase space diagram derived from thermal wind and thermal asymmetry. *Proc 25th Conf Hurricanes and Tropical Meteorology*, San Diego, 29th April–3rd May, 2002, American Meteorological Society, pp 45–46
- Hirst AC (1999) The Southern Ocean response to global warming in the CSIRO coupled ocean–atmosphere model. *Environ Model Software* 14: 227–241
- Holland GJ (1997) The maximum potential intensity of tropical cyclones. *J Atmos Sci* 54: 2519–2541
- IPCC (2001) *Climate change 2001 – the scientific basis*. Cambridge University Press, Cambridge, UK 881 pp
- Kattenberg A, Giorgi F, Grassl H, Meehl GA, Mitchell JFB, Stouffer RJ, Tokioka T, Weaver AJ, Wigley TML (1996) Climate models: projections of future climate. In: Houghton JT, Meria Filho LG, Callander BA, Harris N, Kattenberg A, Maskell K (eds) *Climate change 1995: the science of climate change*, Cambridge University Press, Cambridge, UK, pp 285–357
- Knutson TR, Tuleya RE (1999) Increased hurricane intensities with CO<sub>2</sub>-induced warming as simulated using the GFDL hurricane prediction system. *Clim Dyn* 15: 503–519
- Knutson TR, Tuleya RE, Kurihara Y (1998) Simulated increase of hurricane intensities in a CO<sub>2</sub>-warmed world. *Science* 279: 1018–1020
- Knutson TR, Tuleya RE, Shen W, Ginis I (2001) Impact of CO<sub>2</sub>-induced warming on hurricane intensities as simulated in a hurricane model with ocean coupling. *J Clim* 14: 2458–2468
- Krishnamurti TN, Correa-Torres R, Latif M, Daughenbaugh G (1998) The impact of current and possibly future sea surface temperature anomalies on the frequency of Atlantic hurricanes. *Tellus* 50A: 186–210
- McGregor JL, Walsh KJ, Katzfey JJ (1993) Nested climate modelling. In: Jakeman AJ, Beck MB, McAleer MJ (eds) *Modelling change in environmental systems*. Wiley, Chichester, UK, pp 367–386
- Nguyen K-C, Walsh KJE (2001) Interannual, decadal and transient greenhouse simulations of tropical cyclone-like vortices in a regional climate model of the South Pacific. *J Clim* 14: 3043–3054
- Pielke RA Jr, Landsea CW (1998) Normalized Atlantic hurricane damage 1925–1995. *Weather Forecast* 13: 621–631
- Royer J-F, Chauvin F, Timbal B, Araspin P, Grimal D (1998) A GCM study of the impact of greenhouse gas increase on the frequency of occurrence of tropical cyclones. *Clim Change* 38: 307–343
- Shapiro LJ (1987) Month-to-month variability of Atlantic tropical circulation and its relationship to tropical cyclone formation. *Mon Weather Rev* 115: 2598–2614
- Sugi M, Noda A, Sato N (2002) Influence of the global warming on tropical cyclone climatology: An experiment with the JMA global model. *J Meteorol Soc Jpn* 80: 249–272
- Tonkin H, Landsea C, Holland GJ, Li S (1997) Tropical cyclones and climate change: a preliminary assessment. In: Howe W,

- Henderson-Sellers A (eds) Assessing climate change: results from the Model Evaluation Consortium for Climate Assessment. Gordon and Breach, Australia, pp 327–360
- Tsutsui J-I (2002) Implications of anthropogenic climate change for tropical cyclone activity: a case study with the NCAR CCM2. *J Meteorol Soc Jpn* 80: 45–65
- Tsutsui J-I, Kasahara A (1996) Simulated tropical cyclones using the National Center for Atmospheric Research community climate model. *J Geophys Res* 101: 15,013–15,032
- Walsh KJE, Katzfey JJ (2000) The impact of climate change on the poleward movement of tropical cyclone-like vortices in a regional climate model. *J Clim* 13: 1116–1132
- Walsh KJE, Ryan BF (2000) Tropical cyclone intensity increase near Australia as a result of climate change. *J Clim* 13: 3029–3036
- Walsh KJ, Watterson IG (1997) Tropical cyclone-like vortices in a limited area model: comparison with observed climatology. *J Clim* 10: 2240–2259
- Yoshimura J, Sugi M, Noda A (1999) Influence of greenhouse warming on tropical cyclone frequency simulated by a high-resolution AGCM. Proc 23rd Conf Hurricanes and tropical meteorology, 10–15 January 1999, Dallas, American Meteorological Society, pp 1081–1084